PRINT ISSN 1119-8362
Electronic ISSN 2659-1502

Full-text Available Online at
https://www.ajol.info/index.php/jasem
http://www.bioline.org.br/ja

J. Appl. Sci. Environ. Manage.
Vol. 27 (5) 893-898 May 2023

Evaluation of the Impact of Urban Forestry on Urban Heat Island

***UKOHA, PA; OKONKWO, SJ; ADEWOYE, AR**

Remote Sensing of Tropical Ecosystems and Climate Change Modelling Group.
Forestry Research Institute of Nigeria.

**Corresponding Author Email: ukoha.pa@frin.gov.ng*
Co-Authors Email: okonkwo.sj@frin.gov.ng; adewoye.ralph@frin.gov.ng

ABSTRACT: The purpose of this study is to statistically evaluate the impact of urban forestry on urban heat Island in Umuahia city, located in Eastern Nigeria using Land Surface Temperature (LST) time series. The LST datasets were extracted from the Moderate Resolution Imaging Spectroradiometer (MODIS, MYD11A2 V6) satellite using Python and JavaScript in Google Earth Engine (GEE) platform. Two microclimate environments were considered namely: The Densely and sparsely populated areas in three different locations each. Each microclimate location had 976 observations starting from the 18th of February 2000 to the 1st of May 2021. The Auto-regressive Moving Average (ARMA) was used to model and predict the time series future points of each location; accuracy was measured using Mean Absolute Percentage Error (MAPE) and Root Mean Square Error (RMSE). The Land surface temperature of each selected microclimate location were monitored and the results showed an average observed temperatures difference of 2.9^0C between the Densely Populated and Sparsely Populated areas. In conclusion, the study showed that inhabitants of densely populated areas experience higher temperature regime than the inhabitants living within the sparsely populated areas. This increase in temperature within the densely populated could be attributed to the gradual loss of vegetation cover, which is due to man-made activities such as land use, land cover changes, industrial activities, vehicular movements, and the heat generated from buildings within the city. Thus, a spatial development planning strategy, which controls the growth of the built area and add green spaces should be created for a friendly urban environment.

DOI: **https://dx.doi.org/10.4314/jasem.v27i5.1**

Cite this paper as: UKOHA, P. A; OKONKWO, S. J; ADEWOYE, A. R. (2023). Evaluation of the Impact of Urban Forestry on Urban Heat Island in Umuahia City, Abia State, Nigeria. *J. Appl. Sci. Environ. Manage.* 27 (5) 893-898

Keywords: Auto-regressive Moving Average; Google Earth Engine; Microclimate; Urban Forest

Climate change is one of the most critical challenges that the world faces. Studies have shown that climate change and Urban Heat Island are interrelated (Hansen, 2010). Temperature rises are synonymous with climate change and the resultant effects of increase in temperature is the increase in energy consumption. The energy absorbed by urban surface areas are generated by anthropogenic activities such as the release of energy from air conditioning systems, energy emissions from industrial activities, motor vehicles, the ratio of the number of mixed surfaces, and the difference in heat capacity of building materials with natural structure. According to (Effat et al., *2014*), field verifications showed that most of the hotspots in urban areas have less green space with more spread of metal roofs, industrial buildings, warehouses, railways, high-density parking lots, and solid waste disposal sites. The expansion of urban areas is considered a significant factor for the change in Land Surface Temperature (Hegazy *et al.*, 2015). Land Surface Temperature (LST) is an indicator for environmental change resulting from anthropogenic induced modifications to the environment thereby causing climate change (Weng *et al.*, 2008). LST is one of the climatic parameters, an important factor in the study of urban climate and is widely used for a variety of environmental studies (Kimura and Shimiru, 1994). Satellite image has proven to be a useful tool for monitoring LST trends and variability. (Li *et al.*, 2013). Time series data and model simulations are the major foundations to understanding the climate change dynamics. Satellite Remote Sensing (SRS) is used in acquiring information of the Earth's surface, subsurface and the atmosphere remotely is an

**Corresponding Author Email: ukoha.pa@frin.gov.ng*

important component of time series climate system observations (Yang *et al., 2013).* Umuahia as well as other large cities with economic activity have experienced a series of environmental changes which is attributed to Urbanization. Urbanization induces changes in the mechanism of the energy balance within urban areas thus giving an increase to temperature rise, thereby contributing to global warming (Tokairin, *et al., 2010*). The objective of the study is to analyse the impact of urban forestry on urban heat Island in Umuahia city, located in Eastern Nigeria using Land Surface Temperature (LST) time series model.

MATERIALS AND METHODS

Study Area: The study area consists of Umuahia North and Umuahia South. It lies between longitudes 7˚23' to 7˚36', and latitudes 5˚26' to 5˚37' (Fig 1). Umuahia has an estimated population of 359,230 with an average annual temperature is 26.0 °C and precipitation averages of 2153 mm

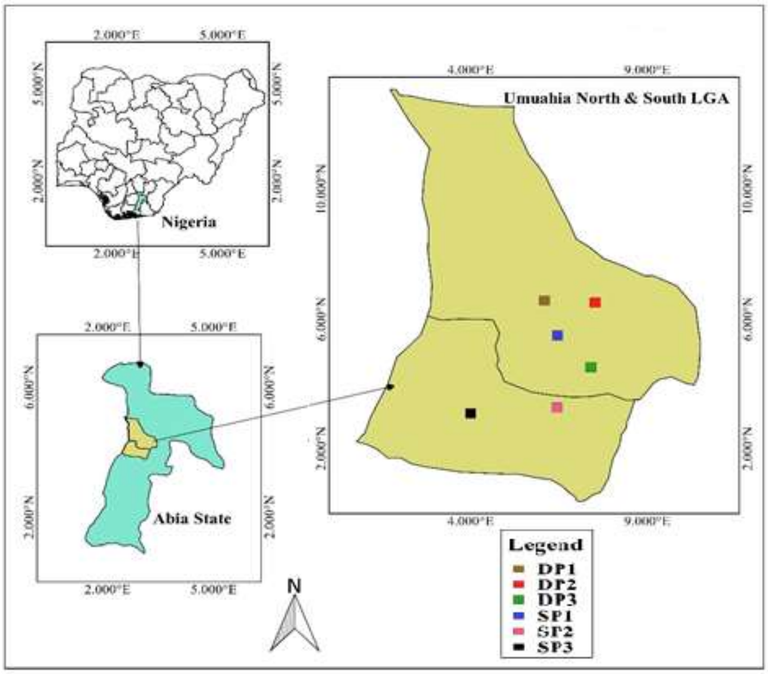

Fig 1: Study Location Map

Data Acquisition: Two microclimate environments were considered namely: The Densely and sparsely populated areas and were stratified into three locations each. Each of the stratified location is a representative of the microclimate environment within the city. At each of the stratified area, five points were randomly selected and Land surface temperature datasets for the stratified areas were extracted from the Moderate Resolution Imaging Spectroradiometer (MODIS) satellite data on the Google Earth Engine (GEE) platform. The MODIS (MYD11A2 V6) is a 1 kilometre (km) spatial resolution satellite data and provides an average 8-day land surface temperature. The stratified location points were used to extract the time series dataset for 21 years (18th February 2000 to 1st June 2021) with a total of 975 observations. The observed data were analysed for the statistical variation using the Autoregressive Moving Average (ARMA) model.

Autoregressive Moving Average (ARMA): The Auto-regressive Moving Average (ARMA) is a statistical analysis model which uses time-series data to predict the future based on past values. ARMA model predicts time series variables by linearly combining their historic values. ARMA models are based on the assumption that past values have some effect on current or future values. This model can be understood by outlining its parameters. These parameters are made up of the autoregressive part which is used to predict variable that regresses on its past values (Shumway and Stoffer, 2010), the integrated part which indicates the stationary of the time series data by subtracting the observations from the previous values (Swain, 2018), the model shows constancy to the time series data over time and the moving average part uses the combination of errors in the past values to predict future variables in a regression-like (Enders, 2004).

Let $X(t)$ be the time series data of interest indexed by some set T, such that

$\{X(t) : t \in T\}$ ------------------------- (1)

and $X_t \in R$. The ARIMA (p, d, q) model – where p is the order of the autoregressive part of the model (Shumway & Stoffer, 2010), d is the degree of differencing, and q is the order of the moving average part of the model – for the time series is given by.

$$(X_t - X_{t-1})^d + \emptyset_1(X_{t-1} - X_{t-2})^d + \ldots + \emptyset_p\left(X_{t-p} - X_{t-p+1}\right)^d = \varepsilon_t + \theta_1\varepsilon_{t-1} + \ldots + \theta_q\varepsilon_{t-q} \ldots\ldots\ldots\ldots\ldots\ldots\ldots (2)$$

This is equal to

$$\left(1 - \sum_{i=1}^{p}\emptyset_i\lambda^i\right)(1-\lambda)^d X_t = \left(1 - \sum_{i=1}^{q}\theta_i\lambda^i\right)\varepsilon_t \ldots\ldots (3)$$

Where ε_t, $\emptyset_i$, θ_i, and λ^i represent the independently and identically distributed error terms of the model, the coefficients of the autoregressive part of the model, the coefficients of the moving average part of the model, and the lag operator respectively. When the time series is stationary, equation () becomes:

$$X_t - \emptyset_1 X_{t-1} - \cdots - \emptyset_p X_{t-p} = \varepsilon_t + \theta_1\varepsilon_{t-1} + \ldots + \theta_q\varepsilon_{t-q} \ldots (4)$$

This is equal to

$$X_t = \sum_{i=1}^{p}\emptyset_i X_{t-i} + \left(1 + \sum_{i=0}^{q}\theta_i\right)\varepsilon_{t-i} + k \ldots\ldots (5)$$

Where$\theta_0 = 1$, and k is a constant term. Equation () is known as the ARMA model. For each location, the derived LST time series observations were divided into a 70/30 ratio for training and validation.

Mean Absolute Percentage Error (MAPE):

Let X_t be the time series data of interest where t is indexed from$\{1, 2, \ldots n\}$, and $X_t \in R$. Let $X_{t_{train}}$ and $X_{t_{test}}$ be subsets of X_t such that$(X_{t_{train}}, X_{t_{test}}) \in X_t$, then $X_{t_{train}}$ is such that $t_{train} = \{1, 2, \ldots, k\}$ and $X_{t_{test}}$ is such that $t_{test} = \{(k+1), (k+2), \ldots, n\}$. Also, let $X_{t_{pred}}$ be the predicted values of X_t indexed from$\{(k+1), (k+2), \ldots, n\}$. The mean absolute percentage error (MAPE) used to measure the accuracy of the predicting method is expressed as:

$$MAPE = \frac{1}{(n-k)}\sum_{k+1}^{n}\left|\frac{X_{t_{train}} - X_{t_{pred}}}{X_{t_{train}}}\right|$$

Here, the absolute value in this calculation is summed for every predicted point in time and divided by the number of fitted points n, multiplied by 100% makes it a percentage error (Myttenaere, 2015). MAPE is a percentage; it can be easier to understand than the other accuracy measure statistics. For example, if the MAPE is 5, on average, the prediction is off by 5%.

Root Mean Square Error (RMSE)

$$RMSE = \sqrt{\sum_{i=1}^{n}\frac{(\hat{y}i - yi)^2}{n}}$$

$\hat{y}_1$, $\hat{y}_2$……$\hat{y}_n$ are predicted values. $y_1, y_2 \ldots\ldots yn$ are observed values, n is the number of observations. Let's imagine that the observed values are determined by adding random "errors" to each of the predicted values, $y1 = \hat{y}i + \in_i$ for $i = 1, \ldots, n$. $\in_{1,\ldots\ldots,} \in_n$ distributed errors. Let's think of $\hat{y}i$ as a distance between X and Y at a particular point in time. The observed yi would be the distance from X to the Y as it is measured with the estimated errors from the mean and standard deviation. RMSE takes the square root of the error and put the metric back in the response variable scale.

$$\sqrt{\mathbb{E}\left[\frac{\sum_{i-1}^{n}(\hat{y}i - yi)^2}{n}\right]} = \sigma^2 + 0^2 = \sigma$$

As n gets larger the variance of $\frac{\sum_i(\hat{y}i - yi)^2}{n} = \sum_i(\mathcal{E}i)^2 / n$ should be converging to zero. RMSE is a good estimator for the standard deviation σ of distributed errors by dividing by n. (Chai, 2014). RMSE is a good way of estimating how good our predictive model is over the actual data, the smaller RMSE the better way of the model fitting. RMSE gives a more accurate value of the error between models and observed.

RESULTS AND DISCUSSION

The data shows that Land surface Temperature (LST) is generally higher in densely populated areas and lower in sparsely populated areas. The statistical data used shows that the LST time series from the different locations were all stationary. The data was observed to have constant mean, variance and autocorrelation with time. The temperature in the densely populated areas was relatively higher (ranging between 30-43^{0}C) and lower in sparsely populated areas (between 29-22^{0}C). Fig 2 shows the Land surface temperature time series datasets for each location.

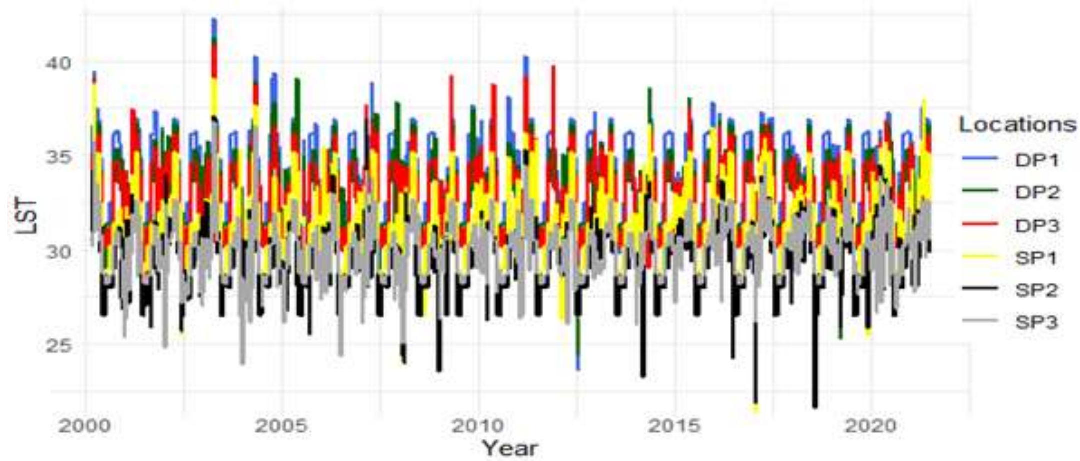

Fig 2: Densely Populated 1 (DP1), Densely Populated 2 (DP2), Densely Populated 3 (DP3), Sparsely *Populated 1 (SP1), Sparsely Populated 2 (SP2), Sparsely Populated 3 (SP3):* Both training and forecasting models were more than 95% accurate. The Root Mean Square Error (RMSE) measures how much error there is between two data sets. In other words, it compares a predicted value and an observed or known value. The smaller an RMSE value, the closer predicted and observed values are. Table 1 shows the mean temperature of each location were calculated and the accuracy, measured using mean absolute percentage error (MAPE). The lower the error, the better the fitness of the model.

Table 1: Mean and Accuracy

Locations	Mean	Forecast Mean	Training MAPE	Test MAPE	Training RMSE	Test RMSE
DP1	33.5648	33.6545	4.0425	5.2567	1.841474	2.967559
DP2	32.9364	32.9727	3.8869	5.1595	1.740295	2.574378
DP3	32.8040	32.9541	3.5440	5.0993	1.589722	2.572569
SP1	31.0830	31.4581	3.5630	5.3902	1.554968	3.428362
SP2	29.5357	29.7301	3.3237	5.1848	1.373546	2.778514
SP3	29.8242	30.1019	2.8901	4.1730	1.206702	2.158915

The Coefficients of Time Series Models shown in table 2 are the Auto-Regressive Integrated Moving Average models for the various locations and each was used to predict future five years temperature scenarios from the year 2020 to 2025 with 95% accuracy. In Fig 3, the black line is the observed data while the blue line is the predicted value of one time point for each selected location with a 95% of the confidence interval. The fluxes of energy, mass, and momentum at the city surface control the geographic separation of diverse microclimates within an urban area (Morgan and Myrup 1977). Urban microclimates respond to local land-cover composition and land cover types influence the spatial distributions of land surface temperature (LST). Urban forestry reduces heat islands through evapotranspiration and shading. The canopy cover provided by Urban forestry reduces the penetration of sunlight, thereby reducing the energy storage in the soil. Also, well-vegetated areas show lower air temperatures. Therefore, Urban Forest reduces acts as heat absorbent by reducing air temperature by transpiration. The substitution of vegetation and green areas with artificial, impervious surfaces is one of the anthropogenic factors contributing to higher ambient urban air temperature (Tsoka et al., 2020). Monitoring the urban heat island in the study area, an average observed temperatures difference of 2.9^{0}C was observed between the sparsely populated microclimate location and the densely populated microclimate location.

Table 2: Coefficients of the Time Series Models

	ar_1	ar_2	ar_3	ma_1	ma_2	ma_3	ma_4	ma_5
DP1	-0.0328	0.4633	-	0.5232	0.0042	0.1651	0.1354	-
DP2	-0.0901	0.6026	-	0.5490	-0.1579	-	-	-
DP3	-0.1345	0.4844	-	0.6040	-0.0022	0.1814	0.2402	0.119
SP1	1.8241	-0.8665	-	-1.3453	0.3805	0.0004	-	-
SP2	0.8375	0.9424	-0.8378	-0.3913	-0.9475	0.3762	-	-
SP3	0.7499	-	-	-0.2913	0.1042	-	-	-

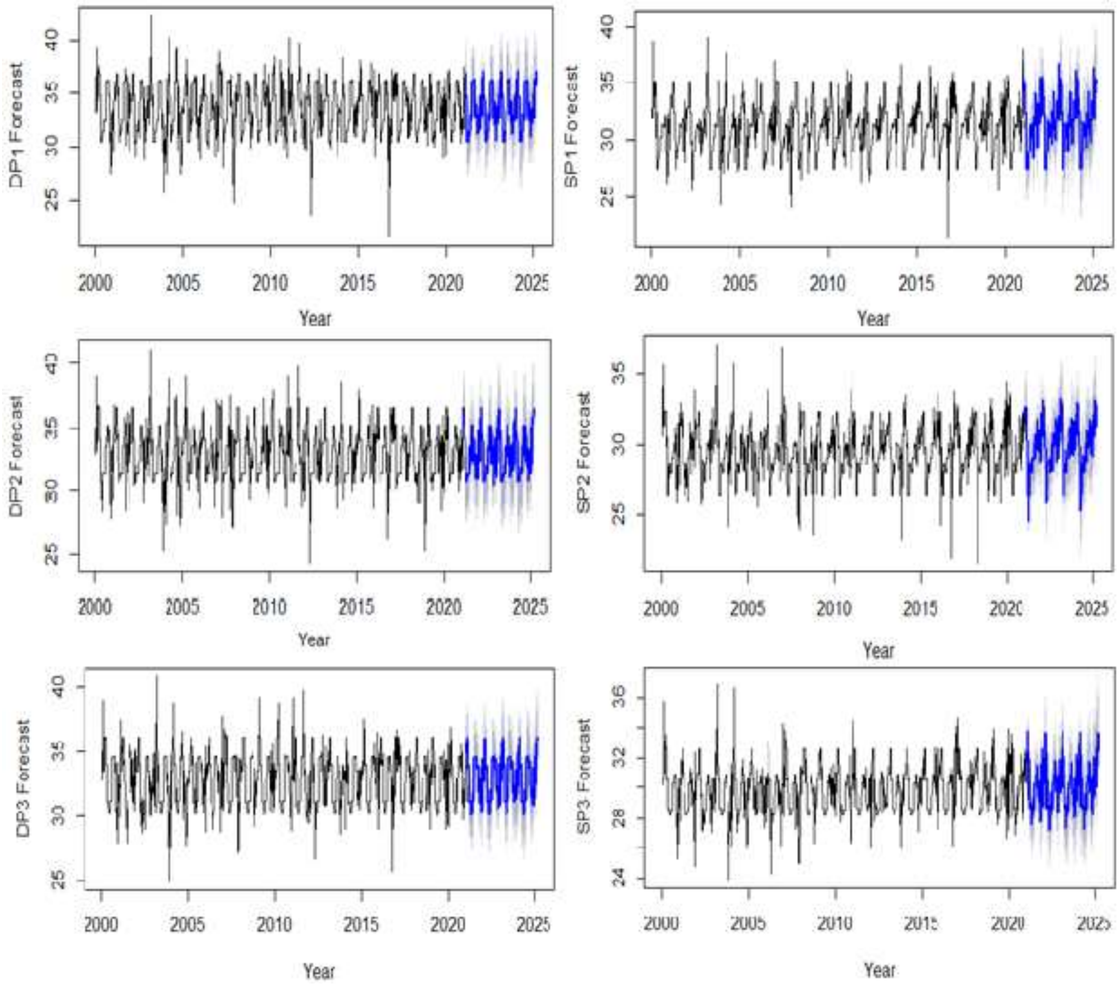

Fig 3: Predicted maps for each location

This difference in temperature between the two microclimate areas can be ascribed to the substitution of vegetation with buildings and hard surfaces (Susca et al., 2011) observed a temperature difference of + 2^0C between vegetated areas in New York City and non-vegetated areas of the city. Studies by (Jenerette et al., 2016; Marc et al., 2010; Coseo and Larsen 2014; Shiflett et al., 2017) observed positive relationships between Land surface temperature and the land cover types. Implications of such studies are not farfetched, anthropogenic induced land cover changes have a monumental effect on urban heat island.

Conclusion: The statistical accuracy analysis between MAPE and RMSE of the land surface temperature distribution measure a good model of fit. The model generates accurate predictions, this shows that anthropogenic activities contribute to the increase in temperature rise. Therefore, it is necessary to develop strategic mitigation between government and scientists to reduce the temperature. This could be achieved by arranging a spatial development plan in urban areas, suitable for its economic, social, and ecological structure for sustainable development.

REFERENCES

Argueso, D; Evans, JP; Pitman, AJ; Di, L (2015). Effects of City expansion on heat stress under climate change conditions. PLoS One, 10 (2).

Berland, A; Shiflett, SA; Shuster, WD; Garmestani, AS; Goddard, HC; Herrmann, DL; Hopton, ME (2017). The role of trees in urban stormwater management. *Landsc. Urban Plan.*162:167-177.

Coseo, P; Larsen, L (2014). How factors of land use/land cover, building configuration, and adjacent heat sources and sinks explain Urban Heat Islands in Chicago. *Landsc. Urban Plan.* 125:117-129.

Chai, T; Draxler, RR (2014). Root Means Square Error (RMSE) or Mean Absolute Error (MAE)? –

Arguments against avoiding RMSE in the literature. *Geosci. Model Dev*.7:1247–1250.

Effat, HA; Hassan, OAK (2014) Change detection of urban heat islands and some related parameters using multi-temporal Landsat images; a case study for Cairo city, Egypt. *Urban Clim*. 10: 171–88.

Enders, Walter (2004). "Stationary Time-Series Models". Applied Econometric Time Series (Second edition.). New York: Wiley. 48–107.

Hansen, J; Ruedy, R; Sato, M; Lo, K (2010). Global surface temperature change. *Rev. Geophys*. 48(4):1-29.

Hegazy, IR; Kaloop, MR (2015). Monitoring urban growth and land-use change detection with GIS and remote sensing techniques in Daqahlia Governorate Egypt. *Int. J. Sustain. Built Environ.* 4(1):117–124.

Jenerette, GD; Harlan, SL; Buyantuev, A; Stefanov, WL; Declet-Barreto, J; Ruddell, JB; Myint, SW; Kaplan, S; Li, X (2016). Micro-scale urban surface temperatures are related to land-cover features and residential heat related health impacts in Phoenix, AZ USA. *Landsc. Ecol*. 31:745–760.

Kimura, Fujio; Shimiru, Y (1994). Estimation of Sensible and Latent Heat Fluxes from Soil Surface Temperature Using a Linear Air-Land Heat Transfer Model. *J. Appl Meteorol. Climatol*. 33 (4):477-489.

Li, ZL; Tang, BH; Wu, H; Ren, H; Yan, G; Wan, Z; Isabel, FT; José, AS (2013). Satellite-derived land surface temperature: Current status and perspectives. *Remote Sens. Environ.* 131:14-37.

Marc, L; Imhoff, P; Zhang, RE; Wolfe, LB (2010). Remote sensing of the urban heat island effect across biomes in the continental USA. *Remote Sens. Environ*. 114 (3):504-513.

Morgan, D; Myrup, L ; Rogers, D; Baskett, R (1977). "Microclimates within an Urban Area." Ann. Assoc. Am. Geogr. 67(1): 55-65.

Myttenaere, AD; Golden, B; Grand, LG; Rossi, F (2015). Mean Absolute Percentage Error for regression models. *Neurocomputing.* 192:38-48.

Tokairin, T; Sofyan, A; Kitada, T (2010). Effect of land-use changes on local meteorological conditions in Jakarta, Indonesia: Toward the evaluation of the thermal environment of megacities in Asia. *Int. J. Climatol*. 30(13):1931 – 1941.

Tsoka, S; Tsikaloudaki, K; Theodosiou, T; Bikas, D. (2020) Urban Warming and Cities' Microclimates: Investigation Methods and Mitigation Strategies—A Rev. Energy. 13(6):1414.

Yang, JP; Gong, R; Fu, M; Zhang, J. Chen, S; Liang, B. Xu, J; Shi, R; Dickinson (2013). "The role of satellite remote sensing in climate change studies." *Nat. Clim. Change.* 3(10): 875-883.

Shumway, R; Stoffer, D (2010). Time series analysis and its applications: with R examples (3rd edition.). Springer.

Susca, T; Gaffin, SR; Dell'Osso, G.R (2011). Positive effects of vegetation: Urban heat island and green roofs. *Environ. Pollut*. 159 (9): 2119-2126.

Swain, S; Nandi, S; Patel, P (2018). Development of an ARIMA Model for Monthly Rainfall Forecasting over Khordha District, Odisha, India. [Advances in Intelligent Systems and Computing] Recent Findings in Intelligent Computing Techniques. 708 (*Proc. of the 5th ICACNI*). 2: 325–331.

Weng, Q ; Liu, H ; Liang, B., Lu, D (2008). Spatial variations of urban land Surface temperatures: pertinent factors, zoning effect, and Seasonal variability. *IEEE J. Sel. Top. Appl. Earth Obs. Remote Sens.* 1(2): 154–166.

Zhou, L ; Dickinson, RE ; Tian, Y; Fang, J; Li, Q ; Kaufmann, R ; Tucker, C; Myneni, R (2004). Evidence for a significant urbanization effect on climate in China. *Proc. Natl. Acad. Sci*. 101(26): 9540–954.